Supplementary information

ATR-FTIR spectroscopy

Data was obtained using a Bruker Vertex 80v FTIR instrument with a PIKE MIRacle™ ATR unit equipped with a ZnSe crystal. 1mg was used to obtain each spectrum. Data was obtained and analyzed using OPUS software with a scan from 600 to 4000 wavenumbers at 2cm^{-1} resolution at 64 scans per spectrum. Both the optical bench and sample chamber were under vacuum (2-5 hPa) for each measurement to remove OH and CO stretching modes from water vapor and carbon dioxide in the atmosphere.

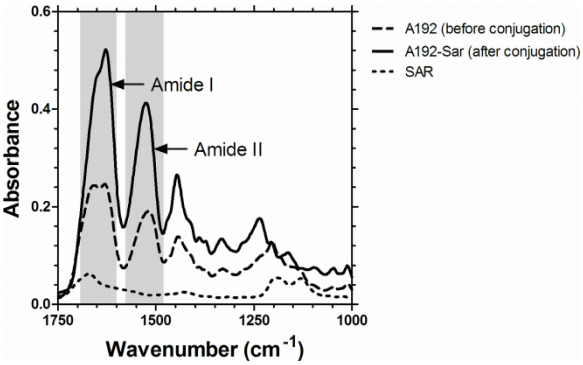

Figure S1 ATR-FTIR spectra of unmodified and modified ELP with the sarcophagine chelator. For comparison the FTIR spectrum of the Sar-chelator by itself is also included.

The conjugation of the sarcophagine cage to the ELP was indirectly confirmed by attenuated total reflection-Fourier transform infrared (ATR-FTIR). Figure S1 shows a comparison between the FT-IR absorbance spectra of A192 and the A192-sar. Two characteristic peaks at ~1665cm^{-1} (amide I, carbonyl stretching) and ~1532cm^{-1} (NH_2 bending and C-N stretching), are observed in both the spectra for A192 and A192-sar. However the ratio of the intensities at ~1532cm^{-1} and ~1665cm^{-1} was higher in A192-sar than on A192, suggesting the reduction of amide I bands due to utilization of the free amine groups of the A192 to form bonds with the carboxyl group of the sarcophagine. This seems to indicate successful conjugation between the chelator and the polypeptide. Peaks at around 1020-1300cm^{-1} are indicative of C-N stretching bands of amines (Saliba et al., Quim. Nova, 35(4):723 [2012]) and are unique to the sarcophagine chelator.

In vitro cytotoxicity

Cytotoxicity testing was performed using the Promega CellTiter 96 Aqueous Non-Radioactive Cell Proliferation (MTS) assay [WI, USA]. The MTS assay is a quantitative and rapid colorimetric method for measuring the viability of cells. The cytotoxicity study of the constructs was examined in vitro on the breast cancer cell line MDA-MB-231; the cell lines were cultured in 96-well plates at an initial concentrations of 3000 cells/well in fresh medium supplemented with 10% FBS. After 24h of culture, cells were adherent and the ELP constructs with and without the Sar conjugate were added at a final concentration of 50µm. The media was removed after 24 h and replaced with fresh medium supplemented with 10% FBS. The cell viability and cytotoxicity were determined using MTS cell proliferation kit. At predetermined time intervals, the MTT reagent was added in each well and incubated for 4 h in a humidified incubator containing 5% CO_2 at 37°C and absorbance was measured at 490 nm using a Perkin Elmer 2103 EnVision Multilabel Plate Reader.

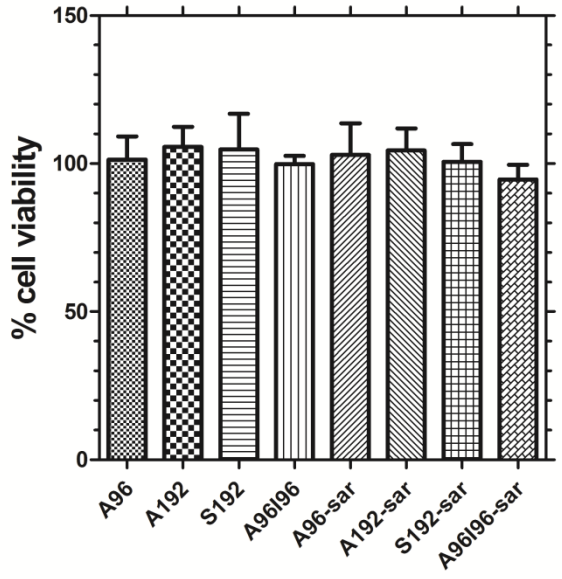

Figure S2 Cell cytotoxicity measured after treatment with ELPs with and without the sarcophagine conjugate 24h incubation. MDA-MB-231 cells were exposed to 50µM of ELP and viability assays (MTS) were performed at 24h. No cytotoxicity is observed in the cells exposed to the ELP constructs. The error bars represent mean ± SD of experiments performed in triplicates.

LCST characterization of ELPs

The LCST characterization of the ELP was determined by measuring solution turbidity as a function of temperature. Solutions of the polypeptide in phosphate buffered saline (PBS) were at a constant rate of 1^{o}c/min in a temperature controlled multicell holder of a UV visible spectrophotometer (DU800 Spectrophotometer, Beckman Coulter, CA, USA). The LCST or transition temperature (T_t) is defined as the point of one half maximal turbidity.

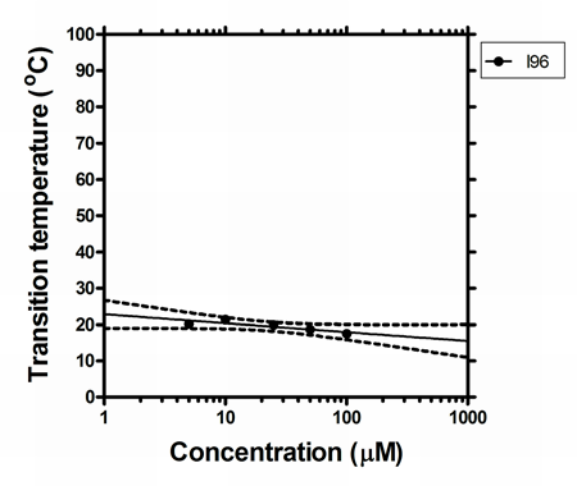

Figure S3 The lower critical solution temperature (LCST) for the isoleucine monoblock with 96 pentameric repeat. The ELP phase diagram was characterized using optical density (350 nm) in phosphate buffered saline as a function of concentration, for which a best-fit line and 95% confidence bands are indicated.

Light scattering characterization

Determination of the hydrodynamic radius of the ELP and ELP-sar conjugates was performed on a Dynapro plate reader (Wyatt Technology Inc., Santa Barbara, CA, USA). The Rh of polypeptides (10 - 100μM) in phosphate buffered saline (PBS) pH 7.4 was determined at 37°C. Before use, the solutions were filtered through Whatman filters with a 0.02μM pore size and centrifuged at 1200 rpm to remove air bubbles.

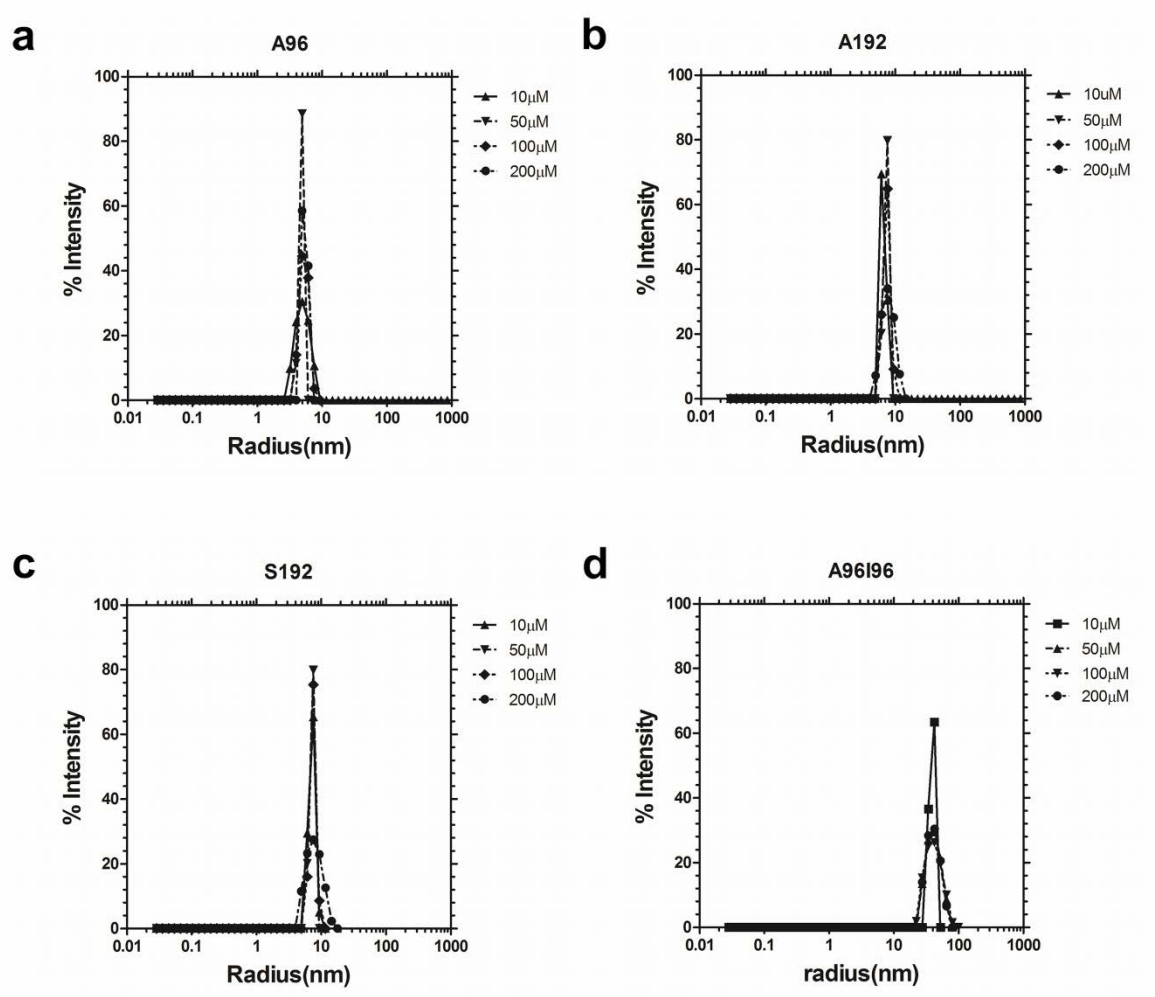

Figure S4 Distribution of hydrodynamic radii is independent of ELP concentration at 37°C. a) A96, b) A192, c) S192, d) A96I96. The regularization fit was reported for each protein polymer at concentrations between of 10-200μM.

An image-drive 6-compartment pharmacokinetic model

A compartmental model (Supplementary Fig. 5) was used to interpret the spatio-temporal data provided by serial microPET imaging of individual mice (Fig. 7, Table 2).

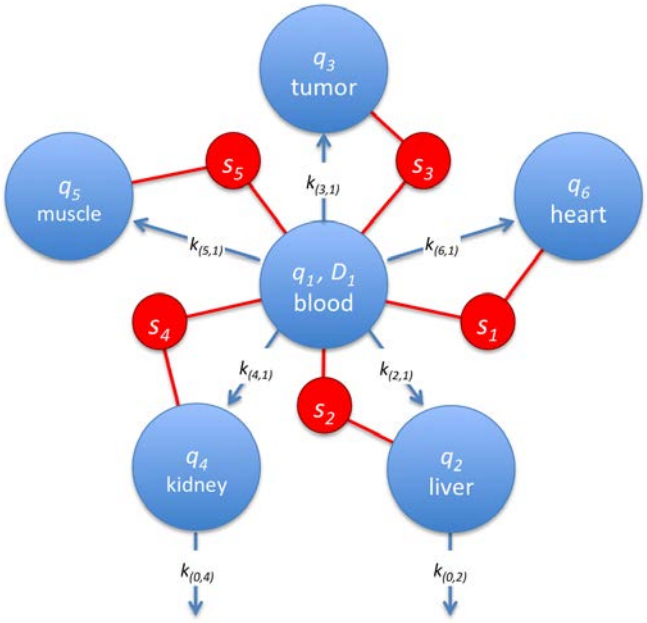

Figure S5. 6-compartment model describing the pharmacokinetics of protein polymer nanoparticles. The model was refined and solved using SAAM II (University of Washington). Compartments (q_1, q_2, q_3, q_4, q_5, *and* q_6) represent a total amount of the initial dose [% ID]. At time = 0, a single bolus dose was administered (D_1) and signal intensities (s_1, s_2, s_3, s_4, *and* s_5) in each tissue [% ID / g body weight (BW)] were fit simultaneously. Based on the structure of this model, the fluxes exiting q_1 represent influx from the blood compartment into the indicated tissue. Sample intensity was defined as the weighted fraction (f_{heart}, f_{liver}, f_{tumor}, f_{kidney}, and f_{muscle}) of signal within the blood plus the signal of material crossing into the tissue via undetermined processes (binding to vascular surface, cellular uptake, extravasation, etc.). During refinement, models including efflux from tissues back into the blood compartment q_1 were considered; however, due to their low magnitude relative to tissue influx, they were neglected without influencing the quality of data fitting. This model as indicated provides a robust fit to each of the individual subjects over the periods imaged (Fig. 7b-e).

Based on the assumptions implied by Supplemental Figure 1, the following equations were used to estimate the relationship between the sample signal intensity and the contributions from both the tissue and intravascular blood:

$$s_1 = \frac{(1-f_{heart})q_6}{m_{heart}} + \frac{f_{heart}q_1}{V_1} \qquad \text{Sup. Eq. 1}$$

$$s_2 = \frac{(1-f_{liver})q_2}{m_{liver}} + \frac{f_{liver}q_1}{V_1}$$ Sup. Eq. 2

$$s_3 = \frac{(1-f_{tumor})q_3}{m_{tumor}} + \frac{f_{tumor}q_1}{V_1}$$ Sup. Eq. 3

$$s_4 = \frac{(1-f_{kidney})q_4}{m_{kidney}} + \frac{f_{kidney}q_1}{V_1}$$ Sup. Eq. 4

$$s_5 = \frac{(1-f_{muscle})q_5}{m_{muscle}} + \frac{f_{muscle}q_1}{V_1}$$ Sup. Eq. 5

Where s_1, s_2, s_3, s_4, and s_5 are the observed signals (% ID/ g BW) in the heart, liver, tumor, kidney, and muscle respectively. q_1, q_2, q_3, q_4, q_5, and q_6 are the total amount (% ID) in the blood, liver, tumor, kidney, muscle, and heart respectively. V_1 (mL) is the apparent volume of distribution for the blood compartment, assuming a density of 1 mg/mL. f_{heart}, f_{liver}, f_{tumor}, f_{kidney}, and f_{muscle} are the fraction of signal contributed by the blood within each tissue for the heart, liver, tumor, kidney, and muscle respectively. m_{heart}, m_{liver}, m_{tumor}, m_{kidney}, and m_{muscle} are the masses of each tissue (g) estimated for the heart, liver, tumor, kidney, and muscle respectively.

$$\frac{dq_1}{dt} = -(k_{(6,1)}+k_{(5,1)}+k_{(4,1)}+k_{(3,1)}+k_{(2,1)})q_1$$ Sup. Eq. 6

$$\frac{dq_2}{dt} = k_{(2,1)}q_1 - k_{(0,2)}q_2$$ Sup. Eq. 7

$$\frac{dq_3}{dt} = k_{(3,1)}q_1$$ Sup. Eq. 8

$$\frac{dq_4}{dt} = k_{(4,1)}q_1 - k_{(0,4)}q_4$$ Sup. Eq. 9

$$\frac{dq_5}{dt} = k_{(5,1)}q_1$$ Sup. Eq. 10

$$\frac{dq_6}{dt} = k_{(6,1)}q_1$$ Sup. Eq. 11

Where $k_{(6,1)}$, $k_{(5,1)}$, $k_{(4,1)}$, $k_{(3,1)}$, $k_{(2,1)}$, $k_{(0,2)}$, and $k_{(0,4)}$ represent the first-order kinetic rate constants for the fluxes indicated in Supplemental Figure 1.

$$Cl_{renal} = V_1 k_{(4,1)}$$ Sup. Eq. 12

$$Cl_{hepatic} = V_1 k_{(2,1)}$$ Sup. Eq. 13

$$Cl_{total} = V_1(k_{(2,1)} + k_{(3,1)} + k_{(4,1)} + k_{(5,1)} + k_{(6,1)})$$ Sup. Eq. 14

Where Cl_{renal}, $Cl_{hepatic}$, *and* Cl_{total} represent the blood clearance (loss from compartment 1) due to accumulation in the kidneys, liver, and total loss to all tissues respectively.

$$t_{half,blood} = \frac{\ln(2)}{k_{(2,1)}+k_{(3,1)}+k_{(4,1)}+k_{(5,1)}+k_{(6,1)}}$$ Sup. Eq. 15

Where $t_{half,blood}$ represents the estimated half-life for material in the central blood compartment. The resulting values for the above parameters are presented in Table 2.